J Electroceram (2009) 22:291–296
DOI 10.1007/s10832-007-9394-x

Optimizing design of the microstructure of sol–gel derived $BaTiO_3$ ceramics by artificial neural networks

Huiqing Fan · Laijun Liu

Received: 27 March 2007 / Accepted: 11 December 2007 / Published online: 23 December 2007

Abstract Modeling and application of artificial neural network (ANN) technique to the formulation design of $BaTiO_3$-based ceramics were carried out. Based on the homogenous experimental design, the results of $BaTiO_3$-based ceramics were analyzed using a three-layer back propagation (BP) network model. Then the influence of sintering temperatures, holding time, donor additives (La_2O_3, MnO_2, Ce_2O_3) and sintering aids (Al_2O_3–SiO_2–TiO_2 (AST)) on the average grain size (d_a), the degree of grain uniformity given by the ratio of the maximal grain size to the average grain size (d_{max}/d_a), and the relative density (D_r) of doped $BaTiO_3$ ceramics system was investigated. The optimized results and experiment data were expressed and analyzed by intuitive graphics. Based on input data and output data, the sintering behavior of $BaTiO_3$ nano-powder was explained well. Furthermore, the fine and uniform microstructure of sol–gel derived $BaTiO_3$ ceramics with $d_a \leq 3$ μm, $d_{max}/d_a \leq 1.20$, and $D_r \geq 98\%$ was obtained.

Keywords Microstructure · Grain size · Sintering · $BaTiO_3$

1 Introduction

Owing to its high dielectric constant at room temperature, stoichiometric submicronised $BaTiO_3$ powders are being widely used for the preparation of dense ferroelectric and piezoelectric bodies, as well as for thin film electronic materials. It is known that the resultant microstructure of the ceramics is one of the key factors for the properties of electronic ceramics. The relative permittivity of $BaTiO_3$ ceramics can be increased to about 3500 if the grain size is controlled at ~1 μm, so a fine-grained structure is desirable to enhance the dielectric performances [1]. Therefore, how to obtain $BaTiO_3$ ceramics with homogeneous and smaller particle size becomes more and more important. However, the grain growth is always difficult to control in the sintering procedure. Many problems may be encountered in processing high-purity stoichiometric and nanocrystalline $BaTiO_3$ powders. Meanwhile, the sintering behavior of $BaTiO_3$ is very sensitive to the sintering temperature, the sintering time, the sintering-aids (e.g. AST), the original powders and the donor additives, and that there may be complex reciprocal actions between them [2–6]. So it is usually difficult to explain their functions in the system. The ever-increasing needs to discover ceramic formulation with a good microstructure requires considerable precise mathematical models in general. It would be intractable for us to develop a reliable modeling for the ceramics without enough knowledge before doing the job by using conventional method.

Due to its remarkable information processing characteristics, the artificial neural network (ANN) has been extensively utilized in solving a diverse area of science and engineering problems. As reviewed by Zupan and Gasteiger [7], ANN seems to be of the most interest, in particular, when a rigid theoretical basis or mathematical relationship is not available in advance. Its application can improve, shorten, or bring new insight into old ways of handling experimental data. In the past decade, there have been numerous successful applications of ANN techniques in diversified areas of science and engineering including

H. Fan (✉) · L. Liu
State Key Laboratory of Solidification Processing,
School of Materials Science and Engineering,
Northwestern Polytechnical University,
Xi'an 710072, China
e-mail: hqfan3@163.com
e-mail: hqfan@nwpu.edu.cn

pattern recognition and classification, voice and image processing, prediction [8], digital communications [9], and nonlinear system identification and control [10]. However, only a few attempts have been conducted ANN on electronic ceramics.

In this work, we used ANN technique to model the sintering behavior of a sol–gel derived $BaTiO_3$-based ceramics. With the aid of ANN model, the optimized design of $BaTiO_3$ ceramics is predicted. The fine microstructure of $BaTiO_3$-based ceramics is obtained by using the optimal parameters.

2 Experimental

2.1 Homogenous experimental design

Doped $BaTiO_3$ nano-powders were prepared by a sol–gel method as shown in Fig. 1. Chemical grade barium hydroxide ($Ba(OH)_2{\cdot}8H_2O$, 99%, Beijing Chemical Factory, China), tetra-butyl titanate ($Ti(C_4H_9O)_4$, 98%, Beijing Chemical Factory, China), additives lanthanum oxide (La_2O_3, 99.5%, Tianjing Chemical Factory, China), manganese oxide (MnO_2, 99.5%, Beijing Chemical Factory, China) and cerium oxide (CeO_2, 99.8%, Tianjing Chemical Factory, China), and sintering-aids (AST) [11] aluminum oxide (Al_2O_3, 99.8%, Luoyang Chemical Factory, China), silicon oxide (SiO_2, 99.5%, Tianjing Chemical Factory, China) and titanium oxide (TiO_2, 98%, Beijing Chemical Factory, China) were used as the starting materials. 2-Methoxyethanol ($CH_3OCH_2CH_2OH$), methanol (CH_3OH) and H_2O were employed as solvents. The preparation of the precursor was a simple process. Firstly, $Ba(OH)_2{\cdot}8H_2O$ was dissolved in the $CH_3OCH_2CH_2OH$. Then, $Ti(C_4H_9O)_4$ was diluted in CH_3OH in a mole ratio of $Ti(C_4H_9O)_4$:CH_3OH= 1:24. At last, $Ba(OH)_2{\cdot}8H_2O$ solution was added into $Ti(C_4H_9O)_4$ solution according to the stoichiometry of Ba:Ti= 1:1. We added well calcined and ground $4Al_2O_3$–$9SiO_2$–$3TiO_2$ powders and then dropped small amount of distilled water after adding nitrate of La^{3+}:Mn^{4+}:Ce^{4+}=1:1:2 under vigorous stirring. The precursor was kept in air at the room temperature for 4 h, yielding a transparent gel. The dried gel, obtained by baking the fresh gel at 120 °C, was calcined at 950 °C for 2 h and milled with carnelian ball for 4 h to form doped $BaTiO_3$ nano-powder in avenge size of 40 nm (Scherrer formula). The calcined powder was die-pressed to green disks in diameter of 10 mm and in thickness of 3 mm at 120 MPa after the addition of a binder. The binder was burned out at 500 °C for 1 h. The green disks were put in a covered Al_2O_3 crucible and were sintered with an electric furnace at 1150~1300 °C for 30~180 min in an air atmosphere. The apparent density of the sintered samples was measured by the Archimedes method of immersion in water. The microstructure of the sintered samples was examined on the polished and thermally etched surfaces by using a scanning electron microscope (SEM; JSM 6460, JEOL Inc., Tokyo, Japan). The grain sizes were determined by the line-intercept method. For knowledge acquisition the homogenous experimental design offers schemes for scientific experimental design within the range of interest. Sixteen formulations gained from homogenous experimental design [12] act as the training data set.

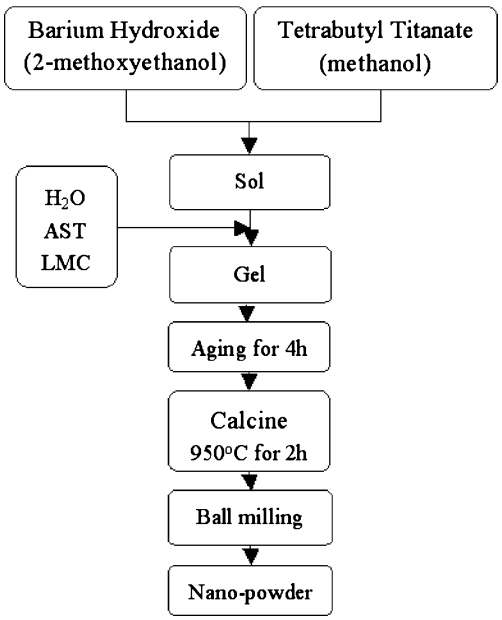

Fig. 1 Flow chart of $BaTiO_3$ nano-powders synthesized by a sol–gel process

2.2 Knowledge acquisition

Because $BaTiO_3$ content is an independent variable among the reagents and the size of original particle is uniform at about 40 nm, the average grain size (d_a), the degree of grain uniformity (d_{max}/d_a), and the relative density (D_r) of doped $BaTiO_3$ ceramics are dependent on mainly sintering temperatures, sintering times, donor additives (La_2O_3, MnO_2, Ce_2O_3) and sintering aids (Al_2O_3–SiO_2–TiO_2, AST). Hence, the ANN model is composed of four neurons in the input layer and three neurons in the output layer. To determine an appropriate number of hidden neurons is an important factor determining the network's performance. From trials using different numbers of hidden neurons 5–10, the minimum in root mean square errors was obtained for six hidden neurons. The architecture of the ANN model is shown in Fig. 2. The initial connection weights are set to be random between 0.3 and −0.3. Within the neural network the learning rate η, the momentum μ and the convergence error are set 0.15, 0.075 and 0.01, respectively.

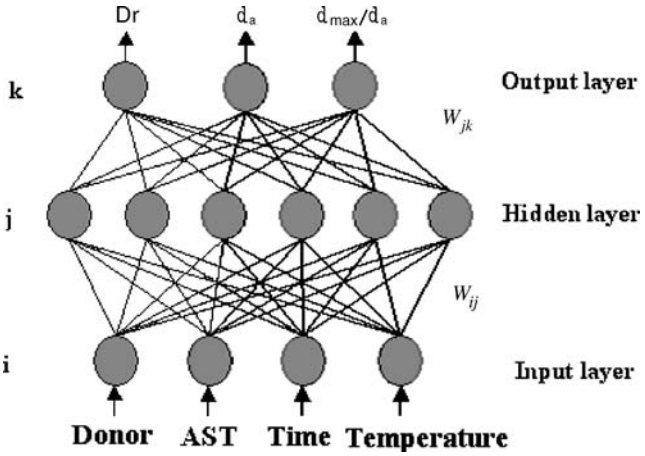

Fig. 2 Architecture of a BP network for the optimizing design of $BaTiO_3$ ceramics

The neuron function is Sigmoid. The maximum iteration is 50000. Table 1 gives the partial training data set. The input data and the output data were normalized to give values between around 0.01 and 1.00.

3 Results and discussion

ANN BP model was trained with the experiment data. On the basis of ANN model, we made use of the method of n-dimensional complex optimization with constraints to calculate the registered $BaTiO_3$ formulation. The finished ANN model is delineated by the connection weights between the input and hidden layers and the connection weights between the hidden and output layers. We saved these connection weights, then for a more convincing inspection of the accuracy of the ANN model, some new samples within the original experimental levels but different from the training samples were also tested. The relationship between observed relative density and calculated relative density for the latter samples is shown in Fig. 3(a), where the two coordinates of a point represent the observed D_r and the calculated D_r of a sample respectively. It is found that the calculated D_r is in good accordance with the observed D_r. These results also indicate that ANN can help us to accurately predict the influence of the sintering process on ceramic microstructures. It should be noted that since decreasing the convergence error can increase the accuracy of the ANN model, however, too small convergence error leads to an over-fitting of the original data points. On the other hand, if the input data are not included in the range of training set, the prediction errors for model might increase dramatically, i.e. the observed values depart from the calculated values. Therefore, for a more convincingly inspection of the accuracy of the ANN model, all input data of simulated samples are not only within the original additives and process levels, but also different from the training samples.

By using a conventional method, it is necessary to do some extra work in order to study the relationship between a processing parameter and microstructure. For example, if we want to study the influence of sintering time on the relative density of the ceramics, we have to fix the sintering temperature, the amount of donor additives and AST then measure the density of the samples dwelling different sintering times. The original experimental data can not be utilized. However, we can express the framework of the model in an intuitive way without any extra experiment by extracting the information of the ANN model registered. Here the graphical analysis capability of the ANN model is also illustrated. The relationship between sintering temperatures and grain sizes, as well as the degree of grain uniformity is shown in Fig. 3(b). The amount of donor additives is 0.4 mol%, AST is 0.1 mol% and the sintering time is 120 min. The average grains size changes linearly with the sintering temperature increasing. It known that the $BaTiO_3$–AST eutectic temperature is 1240 °C [13]. The motion of the grain boundary may be controlled mainly by the pores when the sintering temperature is below 1240 °C. When the sintering temperature is over 1240 °C, although the liquid-phase $BaTiO_3$–AST appears, it does not enwrap grains but mainly exists at the intersection of three grains due to only a little AST sintering-aid. Therefore, the liquid

Table 1 Experimental results of BT ceramic samples.

Sample[a]	1	2	3	4	5	6	7	8	9	10	11	12	13	14	15	16
D_r (%)[b]	86.2	95.9	97.6	87.1	86.9	93.7	83.0	97.5	88.2	95.7	94.6	98.3	94.1	91.3	89.2	96.1
d_a (μm)[c]	2.0	2.9	3.1	2.6	2.3	3.2	1.9	3.1	2.4	2.5	4.0	3.4	4.5	2.4	2.2	2.2
d_{max}/d_a[d]	1.16	1.73	2.47	2.83	1.35	1.72	1.07	2.61	1.01	1.24	3.53	3.81	1.51	3.01	1.04	1.12

[a] The amount of donor additives of La_2O_3–MnO_2–Ce_2O_3 ranges between 0 and 0.6 mol%, the sintering aids of $4Al_2O_3$–$9SiO_2$–$3TiO_2$ (AST) ranges between 0 and 1 mol%, the sintering time ranges between 30 and 180 min, the sintering temperature ranges between 1150 and 1300 °C.
[b] The relative density, measured by the Archimedes method.
[c] The average grain size, determined by the line-intercept method on SEM micrographs.
[d] The degree of grain uniformity, given by the ratio of the maximal grain size to the average grain size.

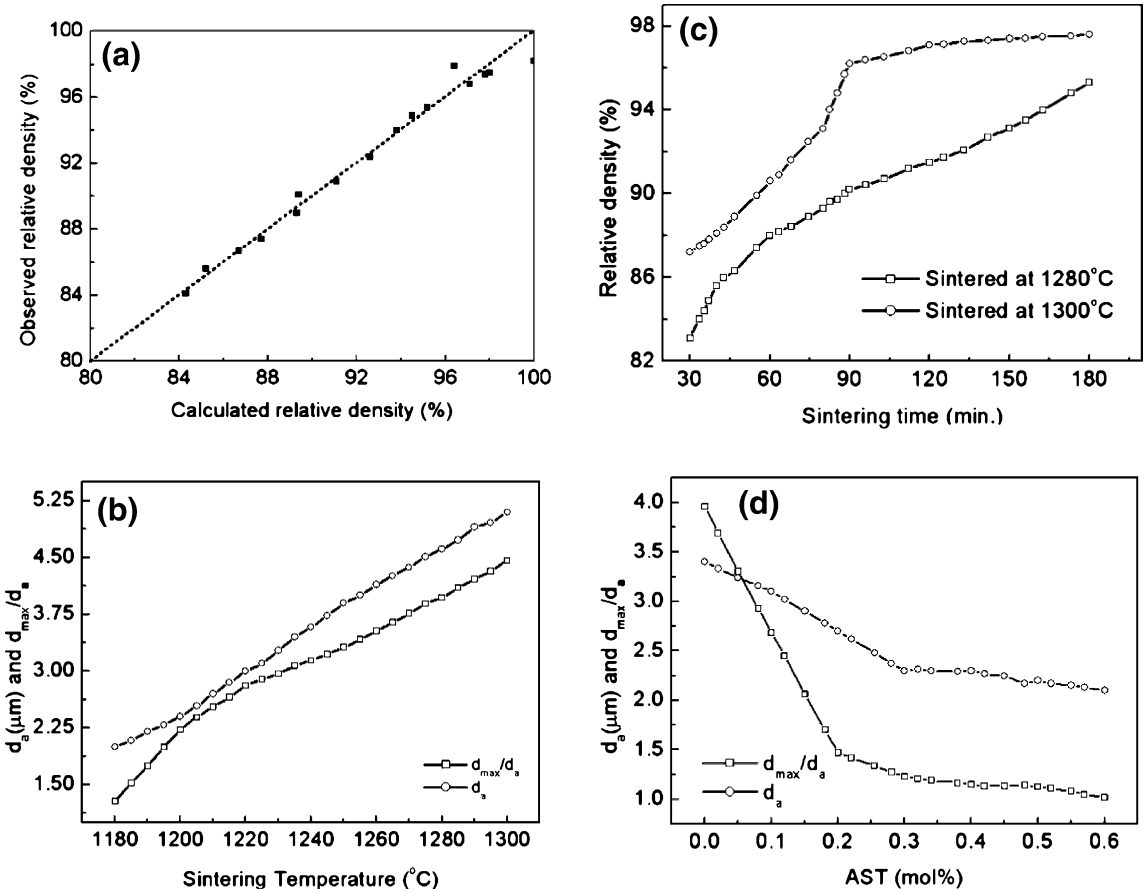

Fig. 3 (**a**) Predicted correlation between the calculated and observed D_r by ANN model, (**b**) relationship between the sintering temperature and d_a, d_{max}/d_a, (**c**) relationship between the sintering time and relative density (D_r), (**d**) relationship between the AST and d_{max}/d_a

phase does not enhance the densification greatly. The sintering temperature dependence of grain size distribution width (d_{max}/d_a) is nonlinear when the sintering temperature is below 1240 °C, but linear at higher temperature. The sintering behavior is against that of powder synthesized by a traditional method. It is suggested that many particles are aggregated. As the sintering temperature increases, some grains become larger at the expense of other grains. By observing the process of grain growth, we also find that Ostwald ripening happens, and some irregular grains appear. In any case, the presence of liquid-phase blocks the motion of grain boundaries and restricts the rate of grain growth so that the grain size does not change acutely at higher sintering temperature.

The relationship between the sintering time and the relative density is shown in Fig. 3(c). The sample, the amount of donor additives is 0.56 mol%, AST is 0 mol%, is sintered at 1280 °C, and the other, the amount of donor additives is 0.56 mol%, AST is 0.1 mol%, is sintered at 1300 °C. It can be seen that bulk shrinkage carries through quickly when the sintering time increases from 30 to 90 min at 1300 °C, but the relative density increases slowly from 90 to 150 min. Finally, the $BaTiO_3$ ceramics in a relative density of 98.3% is obtained at 1300 °C for 180 min. The sintering time dependence of the relative density displays power law behavior when the dwelling time is below 90 min; however, it nearly changed linearly with the increase of sintering time at 1280 °C when the sintering time is above 90 min. Since some particles are aggregated, the densification takes place firstly in the region of hard aggregation. Therefore, the relative density increases quickly as the sintering time increases at 1280 °C with a short dwelling time. As mentioned above, the liquid phase diffusion and grain boundary diffusion generally have an important influence on densification of bulk. It is well known that the liquid eutectic temperature for the TiO_2–$BaTiO_3$ system is 1320 °C for powder synthesized by a traditional method [14, 15]. The liquid eutectic temperature for the TiO_2–$BaTiO_3$ system may be about or less than 1300 °C because the original powders are nanometer powders. When the green disks are sintered at 1300 °C, much liquid phase may appear. The liquid phase distributes well on the grain boundaries and enwraps grains so as to enhance the densification of $BaTiO_3$ ceramics. The sintering intermediate stage finishes when the sintering time is above 90 min. But some isolated pores are left behind, and

then the densification of the bulk carries through slowly by lattice diffusion and grain boundaries diffusion.

The relationship between AST and d_{max}/d_a is shown in Fig.3(d). The AST addition acts not only as the liquid-phase formers to enhance the sintering performance but also as useful contributors to the electron traps at the grain boundary [16]. In this work, the AST plays the role of a sintering aid to enhance the densification and prevent the abnormal grain growth by forming liquid phase. It can be seen that the dependence of the average grain size on the AST is linear below 0.4 mol%. Meanwhile, the grains become fine as the AST increase. But the influence is limited when the AST is above 0.4 mol%. The relationship between AST and the degree of grain uniformity is linear below 0.3 mol%, and the effect of the AST on grain uniformity is pretty strong, but it is ignorable in a wild scope of AST above 0.3 mol%.

Based on above experimental and analyzing results, we inputted again many groups of combinatorial data into input layer of trained ANN, until the perfect data were outputted. Finally, a group of perfect values with d_a=2.8 μm, d_{max}/d_a= 1.16 and D_r=99.7% was output while the amount of donor additives is 0.6 mol%, AST is 0.4 mol%, the sintering temperature is 1300 °C, and the sintering time is 105 min was inputted. A fine microstructure of doped $BaTiO_3$ ceramics with d_a=3 μm, d_{max}/d_a=1.20, and D_r=98% was obtained using this inputting values. The micrographs of $BaTiO_3$ ceramics are shown in Fig. 4. Figure 4(a) and (b) show the microstructure of $BaTiO_3$ ceramics sintered before optimized process. Figure 4(c) and (d) show the microstructure of $BaTiO_3$ ceramics sintered after optimized process. The grains are more uniform than that of samples sintered before optimized procedure. It is confirmed that ANN can accurately predict the trend and rule in the change of parameters with the concentration of the additives and the sintering processing.

4 Conclusions

ANN model is a relatively new computational tools and methodology associated with nonlinear regression technique. Application of a three-layer BP network modeling of the homogenous experimental results, complex influence rules of the sintering process and additives on the microstructure of $BaTiO_3$-based ceramics are shown clearly through several groups of experiments. The observed relative density is in accordance with the predicted relative density. Both the average grain size and the degree of uniformity were controlled effectively by adjusting sinter-

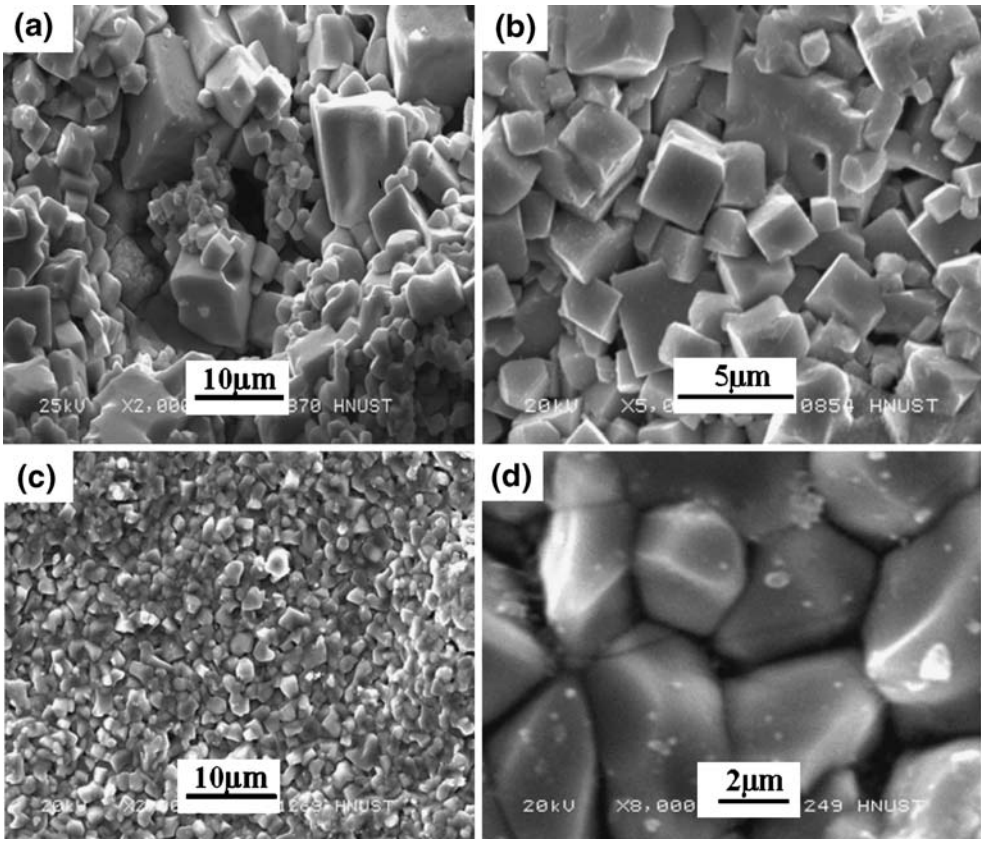

Fig. 4 SEM micrographs of doped $BaTiO_3$ ceramics. (**a**) Sample 4 and (**b**) sample 10 sintered before optimized procedure, (**c**) sample 4 and (**d**) sample 10 sintered after optimized procedure

ing process and additives. Based on input data and output data, the sintering behavior of $BaTiO_3$ nano-powder is explained well, and then $BaTiO_3$-based ceramics with above 98% theoretical density and uniform grains in a size of ~3 μm were successfully sintered by using the group of optimal parameters.

Acknowledgements This work has been supported by the National Nature Science Foundation (50672075) and the Xi'an S&T Research Foundation (GG05015, GG06023, XA-AM-200608), the EYTP and NCET and RFDP (20050699011) Program of MOE, Science Creative Foundation and Doctorate Foundation (CX200704) of NPU, Aeronautic Science Foundation (2006ZF53068) of China. The author, Dr. Huiqing Fan, gratefully acknowledges the support of K. C. Wong Education Foundation, Hong Kong.

References

1. H. Kniepkamp, W. Heywang, Z. Angew. Phys **6**, 385–390 (1954)
2. A. Yamaji, Y. Enomoto, K. Kinoshita, T. Mrakami, J. Am. Ceram. Soc **60**, 97–101 (1977)
3. M. Kahn, J. Am. Ceram. Soc **54**, 452–454 (1971)
4. K.S. Mazdiyasni, L.M. Brown, J. Am. Ceram. Soc **54**, 539–543 (1971)
5. D.A. Payne, H.U. Anderson, J. Am. Ceram Soc **50**, 491–503 (1967)
6. A.C. Caballero, J.C. Fernandez, C. Moure, P. Duran, J. Eur. Ceram. Soc **17**, 513–523 (1997)
7. J. Zupan, J. Gasteiger, *Neural Networks for Chemists: An Introduction* (VCH, Weinheim, Germany, 1993)
8. S. Haykin, *Neural Networks* (Maxwell Macmillan, Ontario, Canada, 1994)
9. J.C. Patra, R.N. Pal, R. Baliarsingh, G. Panda, IEEE Trans. Syst. Man Cybern., Part B, Cybern **29**, 262–266 (1999)
10. J.C. Patra, R.N. Pal, B.N. Chatterji, G. Panda, IEEE Trans. Syst. Man Cybern., Part B, Cybern **29**, 254–256 (1999)
11. Y. Matsuo, M. Fujimura, H. Sasaki, K. Nagase, S. Hayakawa, Am. Ceram. Soc. Bull **47**, 292–297 (1968)
12. K.T. Fang, *Uniform Design and Uniform Design Tables* (Science Press, Beijing, China, 1994)
13. M. Wegmann, F. Clemens, A. Hendry, T. Graule, Ceram. Int **32**, 147–156 (2005)
14. K.W. Kirby, B.A. Wechsler, J. Am. Ceram. Soc **74**(8), 1841–1847 (1991)
15. Y.M. Chiang, D.P. Birnie, W.D. Kingery, *Physical Ceramics* (Wiley, New York, USA, 1997)
16. C.H. Lai, C.T. Weng, T.Y. Tseng, Mater. Chem. Phys **40**, 168–72 (1995)